



DEFORMATION AND DAMPING OF SOIL UNDER TIRES

Thesis of PhD work

Pillinger György

Gödöllő, Hungary

2016

**Doctoral school
Denomination:**

Mechanical Engineering Doctoral School

Science:

Agriculture Engineering

Leader:

Prof. Dr. István Farkas
Professor, DSc
Faculty of Mechanical Engineering
Szent István University, Gödöllő, Hungary

Supervisor:

Prof. Dr. Péter Kiss
Professor, PhD
Faculty of Mechanical Engineering
Szent István University, Gödöllő, Hungary

.....
Affirmation of head of school

.....
Affirmation of supervisor

CONTENTS

1. INTRODUCTION, OBJECTIVES.....	2
2. MATERIAL AND METHOD.....	3
2.1. Measurement methods of traction test.....	3
2.2. Measurement methods of the vehicle	4
2.3. Measurement methods of soil.....	5
2.3.1. <i>Measurement methods and devices of soil surface profiling.....</i>	<i>5</i>
2.3.2. <i>Measurement methods and devices of soil cone index</i>	<i>5</i>
2.3.3. <i>Determination methods and devices of soil physical composition</i>	<i>6</i>
2.3.4. <i>Measurement methods and devices of soil moisture on the field.....</i>	<i>6</i>
2.4. Measurement methods of common parameters	6
2.4.1. <i>Determining the contact patch.....</i>	<i>6</i>
2.4.2. <i>Measurement methods and devices of vibration and traction force... </i>	<i>6</i>
2.5. Measurement methods of soil tank.....	7
3. RESULTS.....	8
3.1. Damping of soil.....	8
3.2. The damping of tire-soil interaction.....	11
3.3. Defining bulk density of the soil with the help of cone index.....	17
4. NEW SCIENTIFIC RESULTS.....	22
5. CONCLUSIONS AND SUGGESTIONS.....	24
6. SUMMARY.....	25
7. MOST IMPORTANT PUBLICATIONS RELATED TO THE THESIS.....	27

1. INTRODUCTION, OBJECTIVES

In my PhD thesis I have aimed to investigate the tire attenuation effect caused by the soil and soil compression. Further goals were defined in order to investigate and reveal physical parameters of the soil. Finally, it was also an aim to create a novel method to define soil density according to load capacity investigations.

My research comprised the following experiments and investigations:

- Field traction experiments on different soil types
- Field soil investigations on untouched and on tire affected soil areas
- Traction experiments on concrete road
- Laboratory experiments on vehicles and tires
- Laboratory experiments on soil
- Experiments in soil tank

According to my experiments and investigations, my research aims to answer the following questions:

- What are the deeper reasons for the occurring dimensions of the tire tracks?
- What are the effects of the initial soil density distribution on the track depth?
- How does soil compresses below the track in function of the density?
- What is the method to calculate the parameter soil attenuation?
- Is it possible to separate the attenuation of the moving tire from the original attenuation?
- Is it possible to define the soil density using measurements with a conical penetrometer?
- What is the mathematical connection between the soil volumetric density and CI index?

2. Material and method

2. MATERIAL AND METHOD

In this chapter, I describe the applied measurement methods and devices. Soil deformation and attenuation investigations were supported by results gathered during field and laboratory experiments.

2.1. Measurement methods of traction test

The investigated vehicle was a Gaz 69 type light truck vehicle, which was towed by a John Deere 6600 type tractor with constant 10 km/h velocity. (Figure 2.1) The traction was performed on concrete road and a dedicated soil type, which was investigated in three different states. The traction device allowed the vehicle to proceed on soil with untouched profile. Tyre pressure was set according to every section of the traction. The settings for tyre pressure were 1,5 bar, 1,8 bar, 2,1 bar and 2,4 bar.



Figure 2.1. Pulling test on arable land: John Deere 6600 and Gaz 69.

For every configuration of tyre pressure a 10 m long, profiled measurement course was defined, where proper acceleration and deceleration sections were also set before and after the measurement course. The investigated vehicle had four identical Taurus 6.50-16 type tires on each wheel.

Table 2.1. Tire stress load capacities, according to catalogue data.

Maximal load to 8,3 m/s (30 km/h) maximal speed:					
78 480 [N/m ²]	98 100	147 150	196 200	245 250	294 300
3041,1 [N]	3433,5	4365,5	5120,8	5787,9	6435,4

The mass of the vehicle was 1310 kg, the front axle stress was 780 kg, the back axle load was 530 kg, the axle distance was 2,38 m, the gage was 1,47 m. The total values are incorporating the mass of the vehicle driver as well.

Measurement steps:

2. Material and method

1. Defining the measurement course (10 m), with run-in and run-out sections.
2. Profiling with communicating vessel-type profiling device
3. Soil sampling, and soil investigations on different points of the measurement track (CI, moisture content of the soil)
4. Setting tire pressure on the investigated vehicle (150 kPa (1,5 bar); 180 kPa; 210 kPa; 240 kPa)
5. Performing traction experiment ($v = \text{const.} = 2,778 \text{ m/s}$, (10 km/h))
6. Re-profiling the measurement course in the tire track (acquisition of remaining profile)
7. Repeating soil investigations in tire track.

The measurement steps were performed on sandy adobe stubble, harrowed (discharrow) and cultivator-tilled. The traction was performed on tarmac as well, without profiling. Table 2.2 defines the parameters for the sandy adobe soil with different states (stubble, harrowed and cultivator-tilled).

Table 2.2. Parameters for the sandy adobe soil with different states.

	Soil density ρ [g/cm ³]*	Water content, n_t [t%]	Load factor k [N/cm ²]	Sand: 2- 0,05 mm	Mud: 0,05- 0,002 mm	Clay: <0,002 mm
Stubble	1,64	16,63	85	90,50%	3,20%	6,30%
Harrowed	1,60	9,46	47			
Cultivator- tilled	1,52	11,10	33			

*average data, distribution is shown in Fig. 3.8

The traction experiments on tarmac were performed to have a reference measurement; the measured data of the soil can be related to the reference (such as contact patch of the tire). The tarmac can be assumed as a non-deformable track, so only the tire suffers deformation during this interaction. The profile of tarmac can be approximated as a planar surface, compared to the investigated soil types.

2.2. Measurement methods of the vehicle

Defining the spring stiffness of the tire

The spring stiffness of the tire can be defined from the recorded spring characteristic at given tire pressure. After setting the required pressure value, the wheel must be relieved. Afterwards, it is required to measure the distance between the center of the wheel and the soil surface (Figure 2.2. a.). Next, the tire

2. Material and method

should be loaded with its own weight. Then different additional weight configurations must be added to repeat the measurements (Figure 2.2.b.). Every weight added 981 N additional load to the investigated wheel. With the increase of the load, the deformation of the tire was also recorded. With an appropriately associated load and deformation values, the spring characteristics of the tire can be defined.



Figure 2.2. Defining the spring stiffness, a) the distance between the center of the wheel and the soil surface, b) extra load on the tire.

2.3. Measurement methods of soil

The type of the investigated soil was sandy adobe soil. The investigated surfaces were: stubble, harrowed, and cultivator-tilled. The investigated parameters of the soil were: soil surface (surface level measuring device), conical index (penetrologger), physical composition, soil sampling, moisture (SMM-1 type soil moisture measuring device). The parameters of soil can differ from each part of the day, so these values were defined directly before and after the measurements. The tarmac course can be assumed to be a totally planar surface.

2.3.1. Measurement methods and devices of soil surface profiling

The soil surfaces before and after each passing were recorded, so that the soil deformation can be calculated precisely. The profiling of the soil surface was performed with a profiler, which works on the principles of communicating vessel. In the highlighted section, the height of the track according to the soil surface was defined at dedicated points, exactly in the middle of the tire tracks.

2.3.2. Measurement methods and devices of soil cone index

The cone index of soil gives information about the load capacity of the soil. It is abbreviated as CI. The CI gives the load capacity of the soil in function of the depth. The CI measurement was performed with a so called Ejkelkamp type penetrometer. The device has a force measuring cell, and a laser type distance meter. With the help of these two modules, the CI is measured and logged in digital form. The measurements were performed in the field, and in a soil tank with (2 cm², 60°) and (3,3 cm², 30°) type, pointed angle pressure probes.

2. Material and method

2.3.3. *Determination methods and devices of soil physical composition*

For the determination of physical composition, soil samples were used, which were directly acquired from the tire track. The samples helped to define the moisture content of the soil, then the particle composition was determined, both for the field soil and the soil tank. The particles were separated with mesh filtering method. With the known amount of the different sized particles, the type of the soil can be determined. With the dimensions of the sampling cylinder, the bulk mass and porosity of the soil can also be determined.

2.3.4. *Measurement methods and devices of soil moisture on the field.*

With the soil samples (and besides the laboratory investigations), the moisture was also determined on the field. A PCE-SMM 1 type moisture measurement device was used with the range of 0 - 50% +/-2%.

2.4. Measurement methods of common parameters

During tire-soil connection, the parameters are formed during the passing of the vehicle, and are affected by the interaction of the vehicle and the soil. An example: a change in the mass of the vehicle will alter the contact patch of the tire. Further changing the load capacity of the soil, or the pressure of the tire, or the spring parameters of the tire may also lead to differences on the contact patch. These changes however also affect the interaction in other different manners as well. The measured parameters (and devices) in the tire-soil interaction are: contact patch (tape line measurement), soil deformation (profiler measurement), traction force (measurement cell), vibration (accelerometer).

2.4.1. *Determining the contact patch*

The contact patch data was measured for every tire pressure and soil state on the front wheels in standing position. When the vehicle boarded onto the given soil type, indicator powder was spread around it, to highlight the surface of the contact patch. When the vehicle moved forward, the remaining area (without the powder) was investigated to measure the length and the width of the area, to calculate the actual contact patch surface.

The surface of the ellipsoid:
$$F_{x,0} = \frac{X Y \pi}{4}. \quad (2.1)$$

2.4.2. *Measurement methods and devices of vibration and traction force*

The vibration was recorded on three different positions of the vehicle, with three different accelerometer devices. An accelerometer with three axes was positioned on the right shaft. An accelerometer with two axes was positioned on the left shaft. An accelerometer with one axis was positioned next to the driver's seat,

2. Material and method

recording vertical vibration. The measured accelerometer data were used without any correction for the actual calculations.

2.5. Measurement methods of soil tank

The soil tank had the following dimensions 1,8 x 1,0 x 0,7 m. The dimensions were determined according to the required distance of the measurement point from the side walls. The CI measurements may be affected by both the side wall and the bottom of the tank. The filling was performed with the same soil types that were used in the field investigations. The soil used to fill up the tank was mesh filtered to remove any floral residues. The tank was filled with two different approaches:

1. Multiple times, with compressed soil of given density. $\rho_6 = 1,65 \text{ g/cm}^3$; $\rho_5 = 1,45 \text{ g/cm}^3$; $\rho_4 = 1,25 \text{ g/cm}^3$; $\rho_3 = 1,1 \text{ g/cm}^3$; $\rho_2 = 0,95 \text{ g/cm}^3$; $\rho_1 = 0,9 \text{ g/cm}^3$.
2. Layered, with compressed soil of different densities (up from the bottom): 10 cm, $\rho_1 = 1,65 \text{ g/cm}^3$; next four layers (5 cm thick), $\rho_2 = 1,45 \text{ g/cm}^3$; $\rho_3 = 1,25 \text{ g/cm}^3$; $\rho_4 = 1,1 \text{ g/cm}^3$; $\rho_5 = 0,95 \text{ g/cm}^3$.

The soil investigations were performed with the aforementioned devices. (CI determination, moisture measurement, bulk density with soil sampling.)

During the measurements two types of cones were used. One cone had an opening angle of 30° with 2,05 cm diameter (meaning $3,3 \text{ cm}^2$ surface), the other had 60° opening angle with 1,6 cm diameter (meaning $2,01 \text{ cm}^2$ surface). The soil provides different responses for different cones with different opening angles.

3. RESULTS

In this chapter I present the deduction processes and the exact novel scientific results obtained from the experiments. According to the literature, I present theoretical deductions in order to analyse and define the parameters of the investigated phenomena, presented in the form of nomograms.

3.1. Damping of soil

The soil compression below the tire bears not only vertical characteristics. Due to the load, sideway creep is occurring in the soil, underneath the pressure surface. For a given sink of the soil (in percentage values for example), a given percentage of sideway creep can be defined. For cohesive soil, this effect has smaller relevance; for soil without cohesion, the effect is more significant.

Relative vertical deformation can be calculated according to the following. According to the soil bulk density, the porosity, and the moisture content:

$$\rho_v = \rho(1 - n_v)(1 - X_n). \quad (3.1)$$

The (3.1) balanced to n_v , if $X_n = 10\%$ and $\rho = 2,7 \text{ g/cm}^3$:

$$n_v = 1 - \frac{\rho_v}{2,4}. \quad (3.2)$$

The change of porosity " n_ε " with " ε " relative strain can be defined with:

$$n_\varepsilon = \frac{n_v - \varepsilon}{1 - \varepsilon}. \quad (3.3)$$

The (3.2) and (3.3) can be used to form an equation defining the relative strain of the soil, with " ρ_0 " (before compression) and " ρ_ε " (after compression) bulk density parameters:

$$\rho_\varepsilon = 2,4 - 2,4 \left(\frac{1 - \frac{\rho_0}{2,4} - \varepsilon}{1 - \varepsilon} \right). \quad (3.4)$$

(3.4) in simplified form:

$$\varepsilon = 1 - \frac{\rho_0}{\rho_\varepsilon}. \quad (3.5)$$

Using (3.5) equation a nomogram can be created to characterize the compression:

3. Results

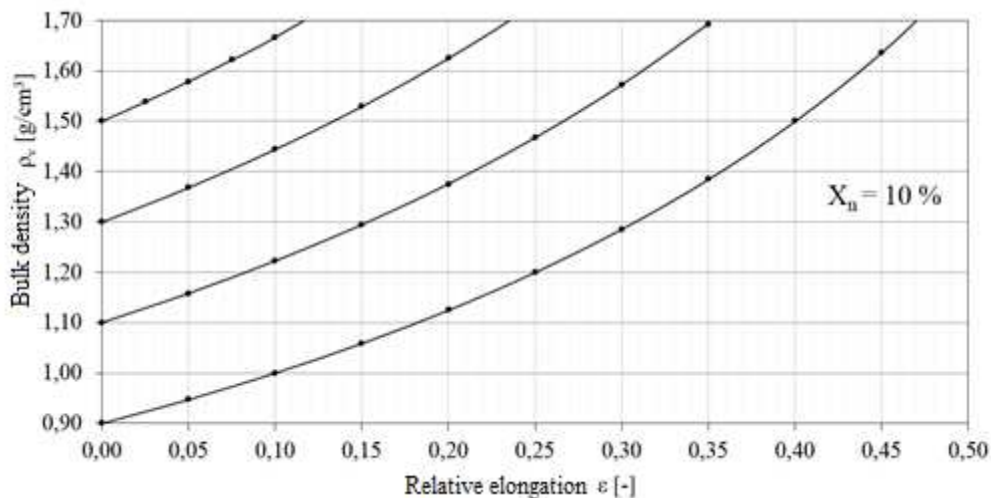


Figure 3.1. Nomogram to determine the relative elongation by bulk density

Determining the load factor of soil

The "k" load factor of the soil can be defined according to the contact patch, and the track depth in the tire-soil interaction. The following equation can be defined according to Szaakjan formula:

$$p = k \left(\frac{z}{d} \right)^n \rightarrow p = \sigma_{\text{köz}} \text{ és } d = d_e; \quad k = \frac{\sigma_{\text{köz}}}{\left(\frac{z}{d_e} \right)^n}. \quad (3.6)$$

The following advantages can be considered when the load factor is determined with the aforementioned method, compared to bevameter investigations:

- There is no need for a large instrument, which would press the pressure plate into the soil.
- The "k" load factor is only independent of "d" diameter, if the "ρ_v" soil density and the modulus of elasticity „E" is constant. This is not a considerable case for the practice. The presented method uses "d" as the diameter of the actual surface.
- Soil deformation under the rolling wheel is in better accordance with reality than the case of vertical pressure plates.
- The only slight disadvantage is that "n" exponent cannot be determined with the track depth of one wheel. To determine the parameter, two

3. Results

wheels with different width are needed. However it is possible to approximate the "n" exponent according to the previously obtained data.

Separation of the damping modes

In the tire-soil interaction damping can be determined with accelerometers fitted on the wheels to record the vibration, and it can be separated into two components. One is the damping of the tire, the other is the damping of the soil. The following deduction presents the separating method of the two components.

The soil load is "F" gives "x₁" tire deformation, and "x₂" soil deformation. According to tire stiffness "K₁" and soil stiffness "K₂":

$$F = K_1 x_1 = K_2 x_2. \quad (3.7)$$

The initial point of the separation is to calculate of the logarithmic decrement, which helps to define "y₂":

$$\delta_{1+2} = \ln\left(\frac{y_0}{y_2}\right) \rightarrow y_2 = \frac{y_0}{e^{\delta_{1+2}}}. \quad (3.8)$$

On the concrete road is the initial and total sinking of the wheel just the tire deformation:

$$\delta_1 = \ln\left(\frac{x_1}{x_{11}}\right) \Rightarrow x_{11} = \frac{x_1}{e^{\delta_1}} = \frac{F}{K_1 \cdot e^{\delta_1}} \quad (3.9)$$

The initial and total sinking of the wheel is the sum of tire and soil deformation:

$$\delta_2 = \ln\left(\frac{x_2}{x_{22}}\right) \Rightarrow x_{22} = \frac{x_2}{e^{\delta_2}} = \frac{F}{K_2 \cdot e^{\delta_2}} \quad (3.10)$$

In the first period:

$$y_0 = x_1 + x_2 = \frac{F}{K_1} + \frac{F}{K_2}. \quad (3.11)$$

In the next period, according to (3.11):

$$y_2 = x_{11} + x_{22} = \frac{F}{K_1 \cdot e^{\delta_1}} + \frac{F}{K_2 \cdot e^{\delta_2}} \quad (3.12)$$

Due to (3.8) the (3.11) and (3.12) has to be divided with each other, then using a simplification:

3. Results

$$\delta_{1+2} = \ln \left[\frac{\left(\frac{K_1}{K_2} + 1 \right) e^{\delta_1} e^{\delta_2}}{\frac{K_1}{K_2} e^{\delta_1} + e^{\delta_2}} \right]. \quad (3.13)$$

On the left side of (3.13) the total measured tire and soil logarithmic decrement values are shown. On the right side (next to the soil and tire stiffness) the logarithmic decrement of the tire (which can be determined according to vibration measurement results on tarmac) and the soil logarithmic decrement are shown. (3.13) should be balanced according to δ_2 :

$$\delta_2 = \ln \left[\frac{\frac{K_1}{K_2} e^{\delta_1} e^{\delta_{1+2}}}{\left(\frac{K_1}{K_2} + 1 \right) e^{\delta_1} - e^{\delta_{1+2}}} \right]. \quad (3.14)$$

With the help of the balanced equation a nomogram can be created, which gives the logarithmic decrement of the soil according to the logarithmic decrement of the tire and the soil- and tire spring constants.

3.2. The damping of tire-soil interaction

The tire and the soil vibrates together, so the damping depends on both the tire and the soil. With identical soil states and different tire pressures, different damping occurs. Similar damping affects the tire during the passing of the vehicle on the soil. The combined plot of damping can be defined according to a drop experiment on the given soil. The logarithmic decrement can be defined with calculations according to the plot. The damping plot data of the vertical accelerometer is shown in Figure 3.2. With the plot, and according to equation (3.13), the logarithmic decrement can be calculated. On different soils (according to the damping of the tire and the soil) the vertical vibration is damped differently.

3. Results

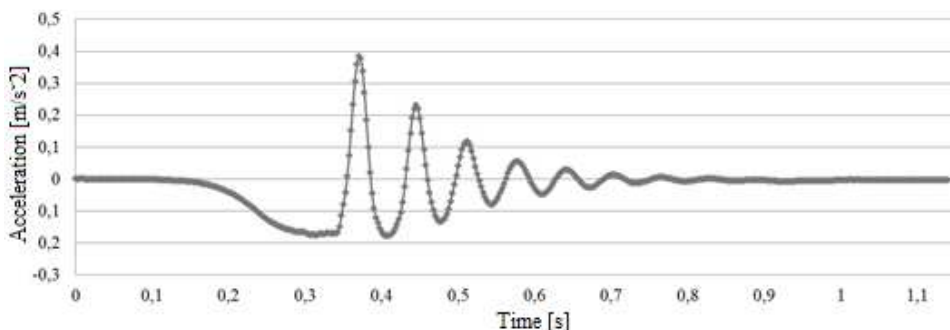


Figure 3.2. Damping plot on stubble, $p_i = 2,1$ bar, $F = 3826$ N, $\delta = 0,58$

The investigations were performed on every soil state and on concrete. The results are shown in Table 3.1.

Table 3.1. Logarithmic decrement of soil-tire interaction, δ [-].

p_i [bar]	Concrete	Stubble	Harrowed	Cultivator-tilled
1,5	0,22	0,35	0,81	1,31
1,8	0,16	0,45	1,02	1,56
2,1	0,12	0,58	1,18	1,85
2,4	0,09	0,72	1,36	2,2

In the followings I take note of the tire-soil interaction parameters; with their help I perform a dimension analysis in order to define new parameters as dimensionless quantities. Every listed parameter was measured or calculated during the experiments.

The parameters affecting the tire-soil interaction are:

1. Load induced by the wheels: $\sigma_{k\ddot{o}z}$, [N/m²]
2. Damping factor: η , [Ns/m]
3. Spring stiffness: K , [N/m]
4. Vibrating mass: m , [Ns²/m]
5. Load factor of soil: k , [N/m²]

3. Results

Table 3.2. The dimension matrix.

	k ₁	k ₂	k ₃	k ₄	k ₅
	η	k	m	K	σ _{köz}
N	1	1	1	1	1
m	-1	-2	-1	-1	-2
s	1	0	2	0	0

No. of variables: 5, no. of dimensions: 3, no. of dimensionless quantities: 2.

After solving the dimension matrix the similarity matrix will be the following:

Table 3.3. The similarity matrix.

	k ₁	k ₂	k ₃	k ₄	k ₅
	η	k	m	K	σ _{köz}
Π ₁	1	0	-1/2	-1/2	0
Π ₂	0	1	0	0	-1

Two dimensionless quantities:

$$\Pi_1 = \frac{\eta}{\sqrt{K m}}, \quad \Pi_2 = \frac{k}{\sigma_{köz}} \text{ vagy } \frac{\sigma_{köz}}{k}. \quad (3.15)$$

According to the previous results a similarity equation can be defined as:

$$\frac{\eta}{\sqrt{K m}} = f\left(\frac{\sigma_{köz}}{k}\right). \quad (3.16)$$

The solution of the similarity equation

The parameters obtained during the field traction experiments can be used to calculate given parameters of the similarity equation. 3.3 Figure shows the results of curve fitting on the calculated points. Tables 3.4, 3.5, 3.6 and 3.7 present the measured initial parameters, which will be used in the following calculations.

Table 3.4. Soil deformation “z” [cm].

p _i [bar]	Concrete	Stubble	Harrowed	Cultivator-tilled
1,5	0	1,7	4,2	6,0
1,8	0	2,2	4,7	6,4
2,1	0	2,6	5,1	6,8
2,4	0	3,1	5,5	7,1

3. Results

Table 3.5. Angular frequency “ ω_0 ” [1/s].

p_i [bar]	Concrete	Stubble	Harrowed	Cultivator-tilled
1,5	7,72	7,32	4,71	3,43
1,8	8,94	5,74	3,86	3,23
2,1	7,54	4,98	3,69	3,02
2,4	9,12	4,12	3,23	2,89

The occurring spring dampness of tire-soil interaction can be calculated according to the eigen-angular frequency, and $m = 390$ kg:

$$\omega_0 = \sqrt{\frac{K}{m}} \rightarrow K = m\omega_0^2. \quad (3.17)$$

Table 3.6. Spring dampness of tire-soil interaction “K” [N/m].

p_i [bar]	Concrete	Stubble	Harrowed	Cultivator-tilled
1,5	228018	205001	84874	45011
1,8	305780	126054	57004	39915
2,1	217509	94884	52094	34894
2,4	318217	64942	39915	31954

The damping factor can be determined according to the measured logarithmic decrement and the eigen-angular frequency. This also points to a correlation between the damping factor and the logarithmic decrement:

$$\eta = \frac{\delta}{\pi} m \omega_0. \quad (3.18)$$

Table 3.7. Damping factor “ η ” [kg/s].

p_i [bar]	Concrete	Stubble	Harrowed	Cultivator-tilled
1,5	211	318	474	558
1,8	178	321	489	626
2,1	112	359	540	695
2,4	102	368	546	790

The load induced by the wheels can be calculated according to the tire load and the contact patch:

$$\sigma_{k\ddot{o}z} = \frac{F}{F_{x,0}}. \quad (3.19)$$

3. Results

Table 3.8. Load induced “ $\sigma_{k\ddot{o}z}$ ” [N/m²].

p_i [bar]	Concrete	Stubble	Harrowed	Cultivator-tilled
1,5	170040	144374	129691,5	115936
1,8	206805	171565	153036	131928
2,1	239119	195199	167803	150035
2,4	273279	218623	182186	163500

The load factor can be calculated for the given soil state with the Szaakjan

formula:

$$p = \frac{F}{F_x} = k \left(\frac{z}{d} \right)^n \rightarrow k = \frac{F}{F_x \left(\frac{z}{d} \right)^n}. \quad (3.20)$$

Table 3.9. The load factor of the soil “k” [bar].

p_i [bar]	Concrete	Stubble	Harrowed	Cultivator-tilled
1,5	0	10	4	3
1,8	0	9	4	3
2,1	0	8	4	3
2,4	0	8	4	3

The diameter of the pressure plate is ”d” in the Szaakjan formula, which is now defined from the equivalent diameter obtained and calculated from the contact patch:

$$d_e = \sqrt{\frac{4F_{x,0}}{\pi}}. \quad (3.21)$$

Table 3.10. Ekvivalent diameter from contact patch „ d_e ” [cm].

p_i [bar]	Concrete	Stubble	Harrowed	Cultivator-tilled
1,5	16,9	18,4	19,38	20,5
1,8	15,3	16,9	17,84	19,2
2,1	14,3	15,8	17,0	18,0
2,4	13,4	14,9	16,4	17,3

Table 3.11. Dimensionless faktor of the load „ $\sigma_{k\ddot{o}z}/k$ ” [-]

p_i [bar]	Concrete	Stubble	Harrowed	Cultivator-tilled
1,5	-	0,15	0,29	0,37
1,8	-	0,20	0,34	0,41
2,1	-	0,24	0,38	0,46
2,4	-	0,28	0,42	0,49

3. Results

Table 3.12. Dimensionless factor of the damping, $\eta/((K m)^{0,5}) [-]$

p_i [bar]	Concrete	Stubble	Harrowed	Cultivator-tilled
1,5	0,0224	0,0356	0,0823	0,1331
1,8	0,0163	0,0457	0,1037	0,1585
2,1	0,0122	0,0589	0,1199	0,1880
2,4	0,0091	0,0732	0,1382	0,2236

With the help of equation (3.22) "η" can be obtained as the combined tire-soil damping factor. With the use of (3.18) the decrement can be denoted in the form of logarithmic decrement. With (3.14) the logarithmic decrement of the soil can be separated from the previous results.

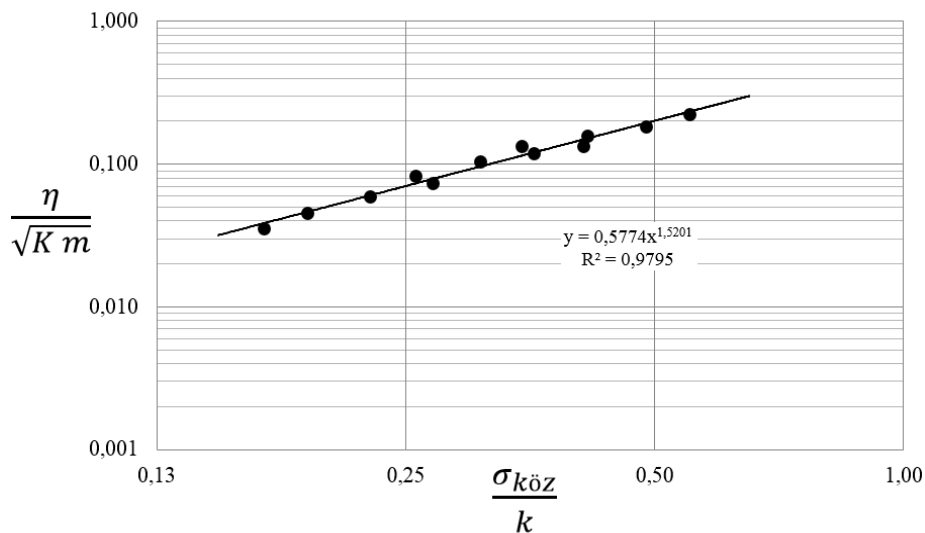


Figure 3.3. The relationship between the dimensionless quantities

The relation between the similarity numbers:

$$\frac{\eta}{\sqrt{K m}} = B \left(\frac{\sigma_{k\ddot{o}z}}{k} \right)^h \quad (3.22)$$

Values of the constants: $B = 0,58 [-]$, $h = 1,52 [-]$.

3. Results

3.3. Defining bulk density of the soil with the help of cone index

The following investigations were performed in controlled conditions, with the help of a soil tank. The same soil was used as in the case of field experiments. The results are presented in Figures 3.4 and 3.5. The results show that interestingly the resistance of the cone was increasing linearly until the depth of 10 cm, then it stabilized at a maximum value. The length of the linearly increasing section exceeded the length of the cone by multiple times. The length of the linear section decreased when the compression increased. This effect raises the difficulty of data evaluation and the practical application of the data to determine the density.

The CI plots and the actual values are depending on the applied cone type. During the measurements the aforementioned (Chapter 2.5) cones were used. To process the CI plots, classical Boussinesq formula for point load should be applied:

$$CI = R \left(\frac{z}{d_k} \right). \quad (3.23) \quad \text{és} \quad CI_{\max} = R \left(\frac{z_{\max}}{d_k} \right). \quad (3.25)$$

Figures 3.4 and 3.5 show the results of penetration experiments for different moisture content. Due to increased moisture the soil becomes more compact, so obtaining data for low densities was not possible.

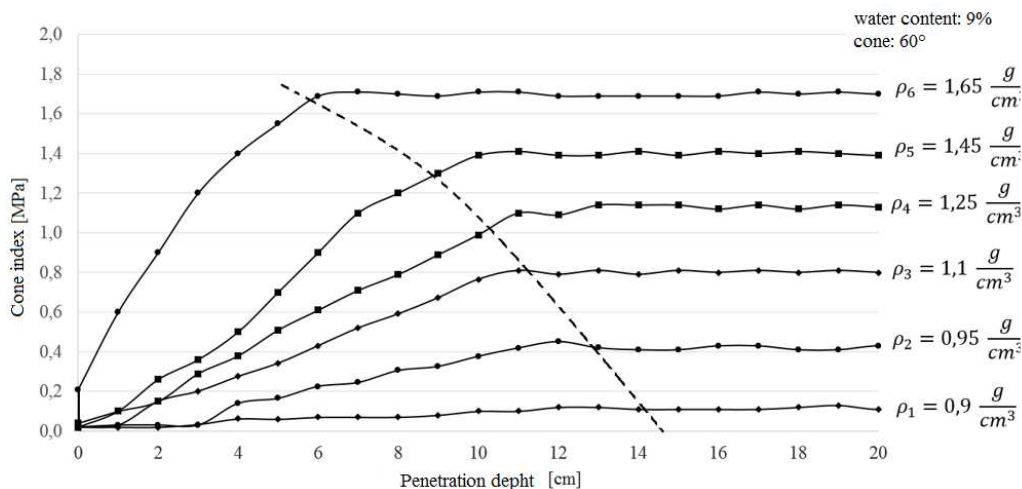


Figure 3.4. Results of penetration experiments in soil tank.

The data obtained from soils with different moisture content show that the breakpoint position aligns to lower penetration depths, as moisture increases.

3. Results

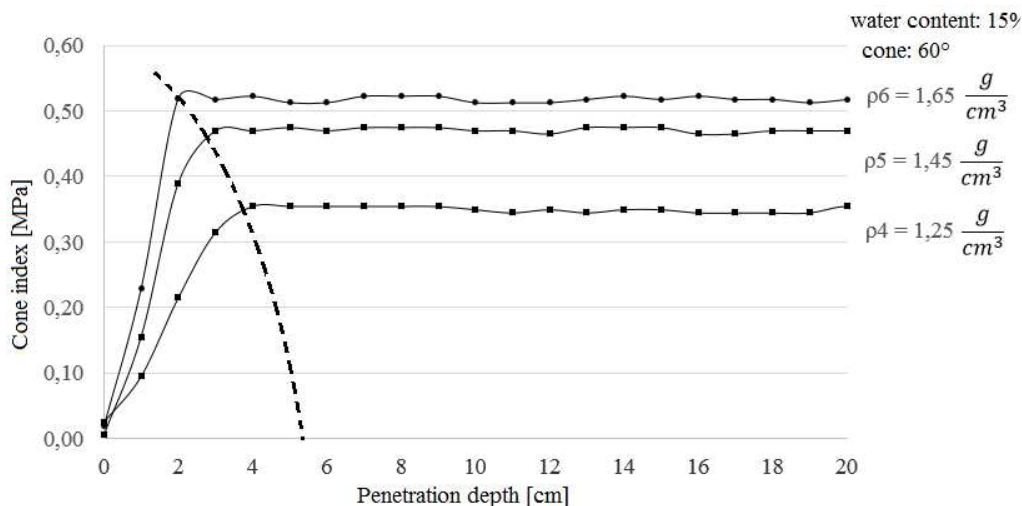


Figure 3.5. Results of penetration experiments in soil tank.

Figure 3.6 shows processed penetration test results (3.4, 3.5) where CI_{max} and R values are presented for the vertical axes at different moisture content cases, in the function of the inverted soil density, presented in logarithmic scale. In this presentation method, the CI_{max} and R values for the same moisture content (also taking note of deviation) are each aligned to given line plots.

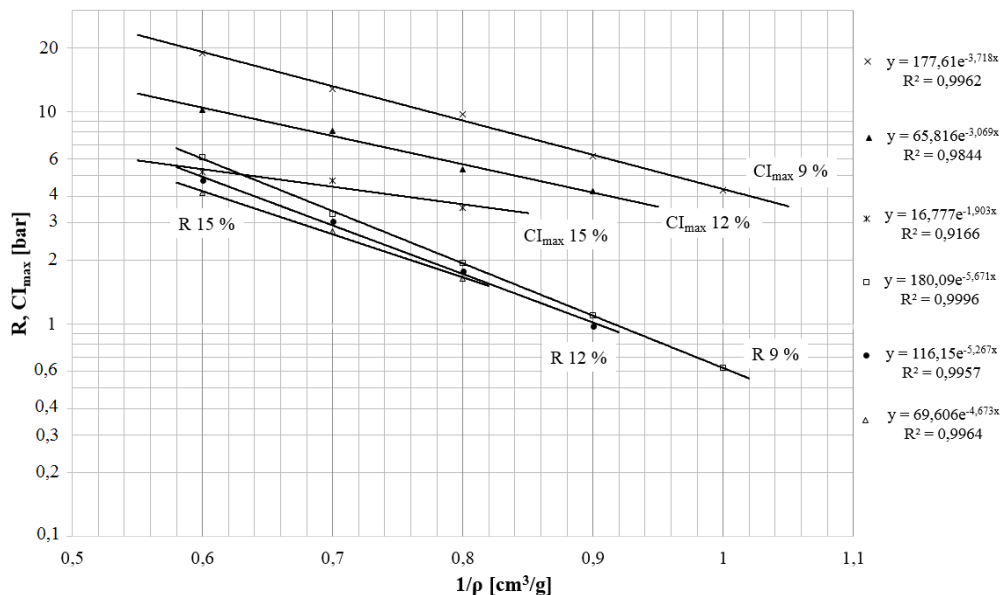


Figure 3.6. The relationship between R , CI_{max} and inverse of soil density

3. Results

The "R" value, which is characterizing the increasing linear section is a negative exponential function, according to the soil density index and the measurements (Fig 3.6):

$$R = A e^{\frac{-B_2}{\rho_v}} \quad (3.26)$$

According to Figures (3.22) and (3.23) the relation between CI and soil density can be deduced from the following (increasing section):

$$\frac{dCI}{dz} d_k = A e^{-B_2 \frac{1}{\rho_v}} \quad (3.27)$$

A division with "A, and both sides must be balanced with the natural logarithm:

$$\ln\left(\frac{dCI}{dz} \frac{d_k}{A}\right) = -B_2 \frac{1}{\rho_v} \quad (3.28)$$

A division with B_2 , then a balancing to ρ_v :

$$\rho_v = \frac{-B_2}{\ln\left(\frac{dCI}{dz} \frac{d_k}{A}\right)} \quad (3.29)$$

Finally it can be assumed that the ln part should be calculated with dCI/dz (in other words the first derivative of CI according to depth) instead of CI/z . On the steady state section, the value of "R" can be calculated according to (3.24).

$$\rho_v = \frac{-B_2}{\ln\left(\frac{CI_{max}}{A}\right)} \quad (3.30)$$

Figure 3.7 shows the CI index of the right track before and after the passing of the wheel. It is observable, that due to the passing of the wheel, CI increased. Density can be calculated according to (3.28). The initial parameters were defined according to the dimensions of the cone and the CI values. Figure 3.8 shows the calculated soil density values according to the depth. The first 2 centimetres are the track depth values. The soil density values after the passing of the wheel are observable only afterwards. Due to the passing (in given layers) the density also increased. The difference calculated from two correlating points (e.g. soil density at 4cm depth before and after the passing) give the extent of compression, which can be defined with relative strain values.

3. Results

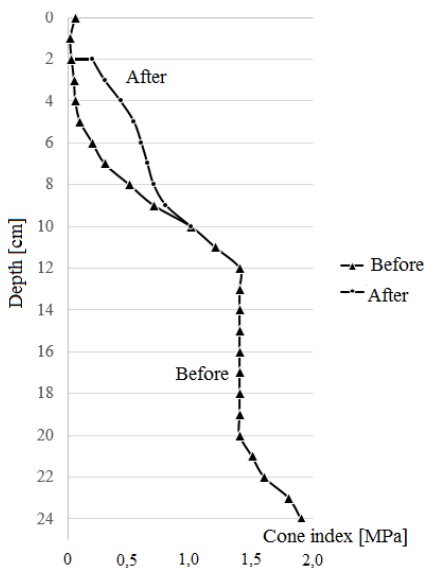


Figure 3.7 Cone index on stubble, before and after the puling test

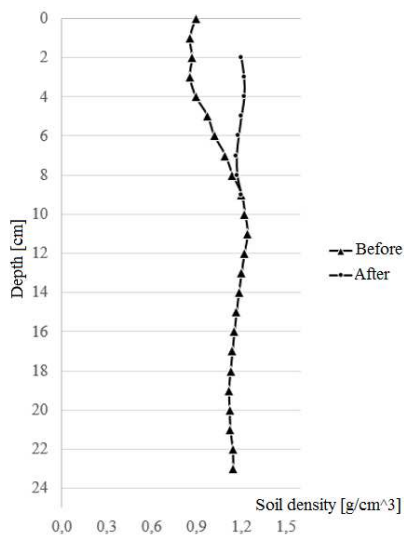
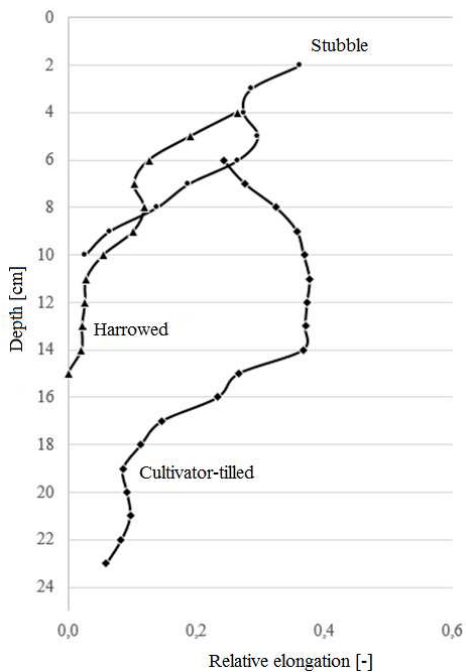


Figure 3.8. Soil density calculated from the cone index data.

With the use of (3.5) and the help of density values, the relative strain of the soil caused by the passing can be calculated for each layer. The relative strain (compression) in function of the depth for the investigated cases are presented in Figure 3.9. The sum of relative strains for each layer give the vertical deformation of the soil without the sideways movement of the layers. The precise inclusion of the latter would require further investigations.

3. Results



According to the previous results it can be stated, that with appropriate experimental data the conical penetrometer is able to approximate the soil bulk density distribution, which may lay the foundations for a more approximate load factor determination.

Figure 3.9. The relative elongation of the soil.

4. NEW SCIENTIFIC RESULTS

1. *Determination of load factor*

I have developed a new method to determine the load factor (k). The method calculates the load factor from the parameters of the track left by the passing vehicle, so that the equivalent diameter obtained from the contact patch is substituted to the pressure plate diameter of the Szaakjan formula. This way the load factor (k) can be calculated with the wheel load and the track depth.

2. *Vibration damping during tire-soil interaction*

I have defined a correlation to define the soil and tire induced damping (η) of a rolling wheel with tire, in dimensionless quantities:

$$\frac{\eta}{\sqrt{K m}} = B \left(\frac{\sigma_{k\ddot{o}z}}{k} \right)^h, \quad \text{or} \quad \eta = B \left(\frac{\sigma_{k\ddot{o}z}}{k} \right)^h \sqrt{K m} \left[\frac{\text{kg}}{\text{s}} \right].$$

To define the damping of vibration, the load induced by the wheels ($\sigma_{k\ddot{o}z}$), the load factor (k), the spring stiffness of the tire-soil interaction (K), the mass of the wheel load (m) and two dimensionless parameters ($B = 0,58 [-]$ and $h = 1,52 [-]$) are required.

3. *Damping effect of soil*

I have defined a correlation for the damping of soil with the resultant logarithmic decrements (δ_{1+2}) of the tire-soil interaction:

$$\delta_2 = \ln \left[\frac{\frac{K_1}{K_2} e^{\delta_1} e^{\delta_{1+2}}}{\left(\frac{K_1}{K_2} + 1 \right) e^{\delta_1} - e^{\delta_{1+2}}} \right].$$

The logarithmic decrement of the soil (δ_2) can be calculated according to the previous results, in the knowledge of the spring stiffness of the tire and the soil (K_1, K_2) and the logarithmic decrement of the tire (δ_1).

4. *Correlation of Bulk density of soil and conical index*

I have defined a correlation between the conical index (CI) values and the soil density (bulk density) (ρ_v) for the increasing linear section of the plot:

For the steady state section:

4. New scientific results

$$\rho_v = \frac{-B_2}{\ln\left(\frac{dCI}{dz} \frac{d_k}{A}\right)}, \text{ for the constant section: } \rho_v = \frac{-B_2}{\ln\left(\frac{CI_{\max}}{A}\right)} \left[\frac{\text{g}}{\text{cm}^3} \right].$$

To define the bulk density according to the CI, the diameter of the penetrating cone and soil dependent constants are required ($A = 185$ [MPa] and $B_2 = 5,7$ [g/cm³]). It is also required to define a depth for the CI_{\max} values (z_{\max}).

5. CONCLUSIONS AND SUGGESTIONS

Due to the inhomogeneity of the field soil and the content of other interfering particles (floral residues, pebbles) it is suggested to use soil tank for the experiments. The tank is filled with prepared soil (cleaned-filtered, with configured moisture), so the soil tank experiments (e.g. penetration tests) are better for novel scientific formulations due to their lower deviance.

I suggest a novel method to define the load factor of the soil from the track depth of a tire. Compared to classic bevameter measurements, my method is a simplified process to obtain the parameter. Its biggest advantage is that the tire itself is used to define the "k" value, which is in more accordance with reality than a vertically moving pressure plate. With two tires of different width, the "n" exponent can also be defined.

The damping ability of the tire and the spring stiffness are important initial parameters in the kinematic and energetic calculations of a vehicle. Also the given damping and spring parameters of the vehicle should be taken into account during these calculations. These parameters are in serial connection with each other. On the field, the investigated system is supplemented with the damping of the soil, which significantly affects the kinematic and energetic relations of the vehicle. The defined combined tire-soil damping factor " η " can serve as an initial parameter for such calculations.

Damping of the tire and the soil absorbs energy and increases the energy requirements for the movement. The vertical vibrations induced by the soil profile causes additional deformations both in the tire and in the soil. The results of Chapter 4.3 can help to define the absorbed energy in the soil. The obtained results may help deeper understanding on the stray losses of vertical vibrations.

The conical penetrometer results can not only help the exact definition of the soil resistance, but the bulk density can also be defined according to the penetration depth. With the results of Chapter 4.4, the bulk density can immediately be determined on the field, with only a slight interference on the soil itself. Classical bulk density determination methods require sampling of the soil, which causes interfering and possible altering of the original soil states. Also the classical methods take more time, which may result in altered soil states from the aspect of density over the examination time window. With my novel results, precise information can be gained from the change of bulk density, both in function of time, and (in the given region) in optional depth values. The method gives more detailed knowledge on the characteristic of bulk density according to the soil layers.

6. SUMMARY

I designed and performed experimental investigations to realize the goals which were presented in the first section of my dissertation. I have taken into consideration the previous results found in the literature of the field. The experimental investigations ranged from field soil, tire-soil and laboratory soil and tire experiments. I wrote detailed conclusions from the literature in the relevant aspects, which guided my investigations and experiments in the proper direction.

In the „materials and methodology” chapter, I described the different experimental setups, the methods and devices of the realization in details.

The field traction experiments were performed at an appropriate area of Szent István University. The physical composition of the soil was precisely defined. The terrain crossing vehicle used in the experiments was pulled with a John Deere 6600 tractor with a special traction coupling device. The tractions were performed at different states of the soil and different tyre pressure setups. The tire parameters (such as spring stiffness of the tire) were measured in laboratory environment.

The results chapter discusses the detailed description of the experimental results, also highlights the conclusions derived from the aforementioned results. 4.1 sub-chapter is titled “theoretical conclusions”. This chapter presents deductions, which can point to new scientific results on their own, also these deductions help faster processing of the measured data, e.g. with the help of assisting plot diagrams. Such diagram is the nomogram of 4.1, which helps reading the relative elongation (compaction) with the known volumetric soil masses before and after the compaction.

With the results of the realized experiments and investigations, four new scientific results were presented in the field of soil compaction and attenuation:

I propose a new method for the definition of carrying capacity parameter of the soil, which have numerous advantages over the currently used methods.

I have created a new computational and describing method to define the damping parameters of the soil. I have specified the damping for the investigated soil, which can be denoted by the logarithmic decrement.

I have shown the correlation between the CI value and the volumetric density of the soil during cone soil penetration tests.

I detailed the newfound correlations and novel methods - which were unfolded during the experiments - in the conclusions and recommendations chapter.

7. Summary

The obtained results give deeper information and understanding on the phenomenon (soil deformation and damping under tire load). They also help to ground new starting points for further experiments.

Summarizing the work, I was able to answer the questions which were initiated in the beginning of my dissertation.

7. Most important publications related to the thesis

7. MOST IMPORTANT PUBLICATIONS RELATED TO THE THESIS

Referred articles in foreign language

1. Laib, L. - Máthé, L. - **Pillinger, Gy.** (2010): The effects of the off-road vehicle on the soil cohesion and internal friction. Mechanical Engineering Letters, Vol. 4., pp. 73-91. HU ISSN 2060-3797
2. Máthé, L. - Kiss, P. - Laib, L. - **Pillinger, Gy.** (2013): Computation of run-off-road vehicle velocity from terrain tracks in forensic investigations. Journal of Terramechanics, Vol. 50. Issue 1., pp. 17-27. (IF: 0,803*)
3. Máthé, L. - Kiss, P. - Laib, L. - **Pillinger, Gy.**- Magdics, G. (2013): Run-off-road vehicle speed analysis from terrain tracks. Mechanical Engineering Letters, Vol. 10., pp. 81-90. HU ISSN 2060-3797
4. Máthé, L. - **Pillinger, Gy.** (2014): Examination of an overturned towed vehicle. Journal of Tekirdag Agricultural Faculty, Vol. 11. Issue 1., pp. 63-66. ISSN 1302-7050

Referred articles in Hungarian language

5. **Pillinger, Gy.** (2011): Vályogos homoktalaj tereprofil mérése. Járművek és Mobil Gépek online folyóirat (http://www.on-and-off-road-vehicles.hu/pdf/15_152_161.pdf domain név alatt), III. évf., 1. sz., 152-161. o., HU ISSN 2060-4408
6. **Pillinger, Gy.** (2014): Talajdeformáció meghatározása gumiabroncs-talaj kapcsolat reológiai modelljével. Mezőgazdasági Technika, LV. évfolyam, április, 2-5. o., HU ISSN 0026-1890
7. **Pillinger, Gy.** (2014): Függőleges lengések hatására keletkezett járulékos teljesítmény veszteség megoszlása a gumiabroncsabroncs és talaj között. Járművek és Mobil Gépek online folyóirat (http://www.on-and-off-road-vehicles.hu/pdf/pillinger_2014.pdf domain név alatt), VI. évf., 1. sz., 1-7. o., HU ISSN 2060-4408